HiSST: International Conference on
High-Speed Vehicle Science Technology
26–29 November 2018, Moscow, Russia

# Aerodynamic Damping and Buffet Response Test of an Aeroelastic Launch Vehicle Model in Transonic Flow

*Chen Ji[1], Ziqiang Liu, Kui Bai, Feng Li*

## Abstract

The aerodynamic damping and buffet response of a hammerhead launch vehicle were tested at the Mach number of 0.8 to 1.2 and angle of attack of 0° and 8°. The model is aeroelastic scaled with scaled configuration and structural dynamic characteristics. The aerodynamic damping of the model vibrating in the first and second free-free bending mode were measured respectively by exciting the model at the corresponding frequency with an electromagnetic shaker. The aerodynamic undamping was found at the second free-free bending mode at Ma=0.9 and AoA=8°. The buffet response was measured using strain gage bridge located at the middle of the model with only flow turbulence exciting. Both first and second free-free bending modes were excited by the flow. At different Mach numbers, the variation of the peak value of the free-free bending response power spectral density can be up to 14.4 times. Although the second-order aerodynamic damping was zero at Ma=0.9 and AOA=8°, it had a limited effect on the second-order dynamic bending response amplitude in this test condition.

**Keywords**: *aerodynamic damping, buffet response, aeroelastic, transonic, wind tunnel test*

## 1. Introduction

Buffeting of launch vehicles is an important aeroelastic problem area both in terms of the structural loads experienced by the entire vehicle and the local vibration environment in which payloads and instruments may be placed. Therefore, the aerodynamic scaled models were employed to study the dynamic characteristics of the launch vehicles in the wind tunnel test.

Hanson and Doggett [1, 2] developed a technique using flexible models to provide experimental data on the oscillatory aerodynamic damping and buffet load characteristics of slender flexible bodies. The technique can extend to launch vehicles that have much more complicated shapes. M. X. Feng [3] and K. Bai [4] developed an aeroelastic model design technique which using a central aluminium tube with axial slots to simulate the model stiffness distribution. The technique was successfully applied to the aerodynamic damping tests [3,4]. Z. Q. LIU [5,6] established a numerical approach to predict the aerodynamic damping coefficient and studied the mechanism of the transonic aerodynamic undamping. Chen [7] studied the aerodynamic damping of a lunch vehicle on the free-free bending mode in transonic wind tunnel.

In the present investigation, an aeroelastic scaled model of a launch vehicle was designed. The aerodynamic damping of the model vibrating in the first and second free-free bending mode and the buffet response were studied at the angle of attack of 0° and 8° and at the Mach number of 0.8 to 1.05 in the transonic wind tunnel. The aerodynamic damping and buffet response were studied with the experimental data.

## 2. Model design

The aeroelastic scaled model was the model that can simulate the mass, stiffness and aerodynamic characteristics of the full-scale vehicle. The similarity criterions for the aeroelastic wind tunnel test are the mass ratio parameter, reduced frequency and Mach number. The main physical quantities related

[1] *China Academy of Aerospace Aerodynamics, No. 17 Yungang West Road, Fengtai District, Beijing, China, E-mail jichen167@hotmail.com*

to the aerodynamic damping wind tunnel test were dynamic pressure q, mass m, stiffness EI, velocity V, frequency $\omega$, length l, density $\rho$ [8]. According to the dimensional analysis, the density ratio $k_\rho$, the dynamic pressure ratio $k_q$, and the length ratio $k_l$ were regard as basic scale factors. And the stiffness ratio $k_{EI}$, the frequency ratio $k_\omega$and the mass ratio $k_M$ were the induced scale factors. The scale factors used in model design were determined by wind-tunnel size and performance capabilities and by the full-scale trajectory flow conditions.

The scale factors were expressed as follows where subscript F denotes Full-Scale and subscript M denotes Model-Scale:

$$k_\rho = \frac{\rho_F}{\rho_M};\ \ k_q = \frac{q_F}{q_M};\ \ k_l = \frac{l_F}{l_M};\ \ k_{EI} = k_q k_l^4;\ \ k_\omega = k_\rho^{-0.5} k_q^{0.5} k_l^{-1};\ k_M = k_\rho k_l^3$$

The elastic model consisted of a head fairing and an elastic core stage without boosters. The core stage elastic model was a central aluminium tube with axial slots [7]. Variation of the height of the slots and the thickness and radius of the tube provided the property scaled stiffness distribution except for minor deviations because of model structural considerations. Tungsten weights attached to the aluminium tube provided the proper weight distribution. Full-bridge strain gages were mounted at the middle of the model to measure the bending response.

## 3. Model Support and Excitation

The aeroelastic model was sting mounted. It was attached to the sting by leaf springs [7]. The springs were attached to the model near the nodal points of the first free-free bending mode in order to minimize the influence of the springs on the free-free mode. The results of the structural dynamic analysis of the support system showed that the effect of the attachment springs was negligible. An electromagnetic shaker was used to excite the model in its elastic bending modes of vibration in order to determine the aerodynamic damping in each mode. The field coils were attached to the sting and the moving coils were attached to the rear side of elastic core stage.

## 4. Structural Dynamic Characteristics

The ground vibration test was performed to determine the structural dynamic characteristics of the elastic models. The experimental mode shapes were determined by forcing the model with the electromagnetic shaker at the resonant frequency and by measuring the variation along the model of the relative vertical displacement by means of a small accelerometer. The first three vibration modes were supporting modes that due to the flexibility of the connecting leaf springs. The fourth and fifth modes that be excited were the first and second free-free bending modes of the vehicle.

The experimental mode shape of the elastic model and launch vehicle in free-free bending were shown in figure 1 and 2. The MAC (Modal Assurance Criterion) value is 0.95 for the 1st mode and 0.88 for the 2nd mode, indicating a good agreement of the mode shapes between the launch vehicle and the aeroelastic scaled model. The modal frequencies and structural damping of the first and second free-free bending mode were listed in table 1.

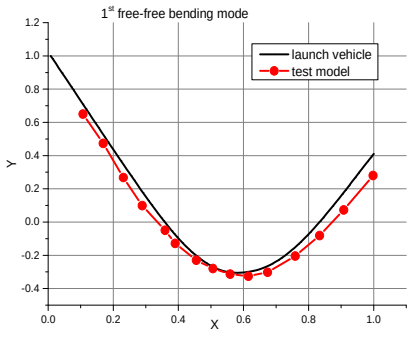


**Fig 1.** Mode Shapes of 1st Free-Free Bending Mode

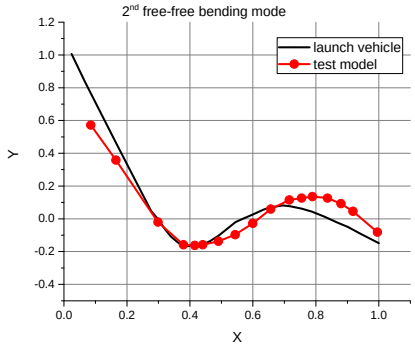


**Fig 2.** Mode Shapes of 2nd Free-Free Bending Mode

**Table 1.** Structural Dynamic Properties of 1st Free-Free Bending Mode

| Mode | Modal Frequency Hz | Structural Damping |
|---|---|---|
| 1st mode | 182.2 | 0.0167 |
| 2nd mode | 391.3 | 0.0191 |

## 5. Wind Tunnel Test

### 5.1. Aerodynamic damping test

The investigation was conducted in the CAAA FD-08 transonic wind tunnel, which has a 530mm× 760mm rectangular test section. With the model mounted in the tunnel and no wind adding on, the electromagnetic shaker was used to excite the model at the resonant frequencies of its free-free bending modes. The model was excited to an amplitude that would be the same as that during the wind-on portion of the test. After obtaining the no-wind data, the wind tunnel started. The tunnel was brought to a desired Mach number, and the model was forced to vibrate at the 1st or 2nd of its free-free resonant frequencies. The total damping data were recorded in the same manner as was done under no-wind conditions. The time responses of the strain gage at different Mach numbers and angle of attacks for the 1st and 2nd free-free bending modes were shown in the Fig 3 to Fig 6. As shown in the figures, the amplitudes when the vibration started were nearly the same. However, the rates of the attenuation of each vibration were different, indicating that the aerodynamic damping was different.

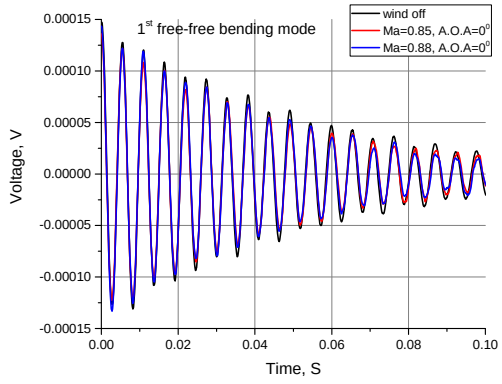


**Fig 3.** Time response (AoA=0°,1st mode)

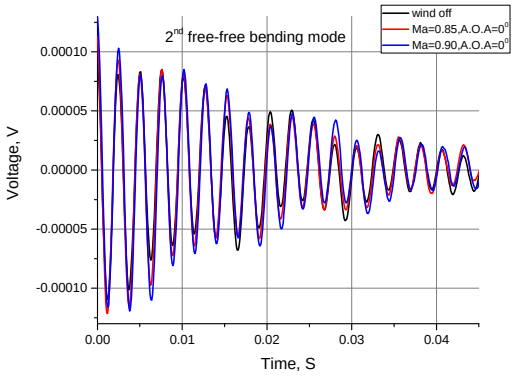


**Fig 4.** Time response (AoA=0°,2nd mode)

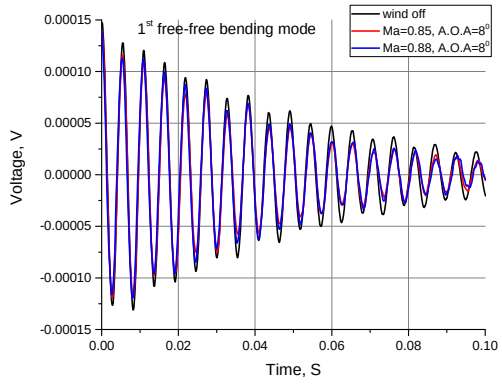


**Fig 5.** Time response (AoA=8°,1st mode)

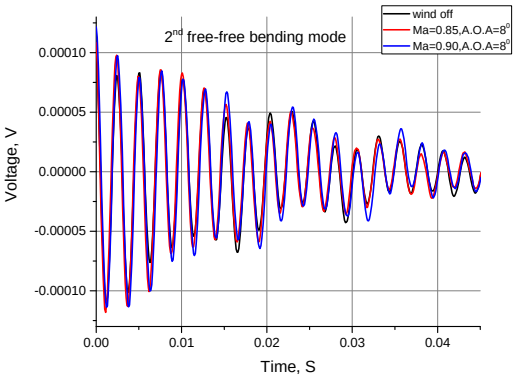


**Fig 6.** Time response (AoA=8°,2nd mode)

The model aerodynamic damping ratio was determined by measuring the total damping with the wind on and subtracting from that value the structural damping ratio determined with the wind off. The

damping ratio of the recorded time domain data was processed by ERA method. The aerodynamic damping of the 1st and 2nd free-free bending mode at different Mach numbers and AoAs were shown in the Fig 7 and 8. The results showed that both Mach number and angle of attack have some effects on the aerodynamic damping of this configuration. As shown in the Fig 7 and 8, the aerodynamic damping dip can be found in both 1st and 2nd free-free bending mode at the two tested angles of attack. The dip was at the Mach number of 0.88 for the 1st mode, and at the Mach number of 0.9 for the 2nd mode. The aerodynamic undamping was found at the second free-free bending mode at Ma=0.9 and AOA=8°, and the aerodynamic damping ratio was $0.0x10^{-3}$.

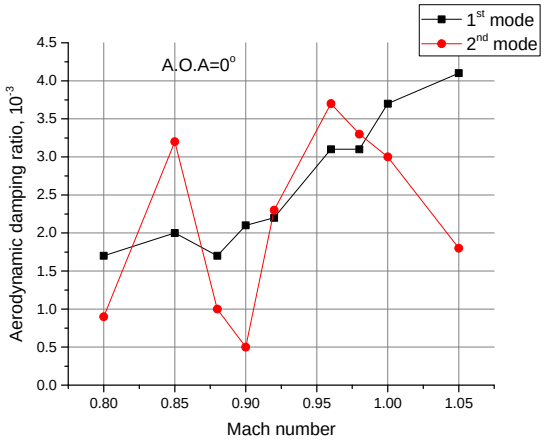


**Fig 7.** Aerodynamic damping of the model at AoA=0°

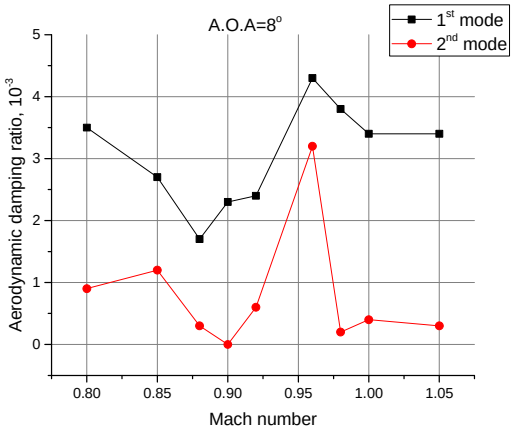


**Fig 8.** Aerodynamic damping of the model at AoA=8°

### 5.2. Buffet response test

The buffet response was tested by measuring the dynamic bending response of the model with the same strain gages used in the aerodynamic damping test. The tests were conducted at the AoA=0° and 8° and the Mach number of 0.8 to 1.05. In the test, the model was excited by the turbulence of the flow without additional exciting. Therefore, the response that measured by the strain gages was only excited by the flow.

The dynamic bending responses at some of the tested Mach numbers are shown in Fig 9 and 10. No significant trend can be read from the figures. The power spectral densities of each tests were calculated for the analysis of the frequency domain characteristics and the energy distribution. As shown in the Fig 11 and 12, there were 5 main modes that were excited, and at this measured location, the main vibrational energy was concentrated between 50 Hz and 200 Hz. Compared with the previous modal test results, the first three modes were not the free-free bending modes of the aeroelastic scaled model but the supporting modes that brought in by the low stiffness of the supporting springs. Therefore, the 4th and 5th mode in Fig 11 and 12 were the 1st and 2nd free-free bending mode of the model, respectively.

Fig 13 and 14 show the power spectral densities of the 1st and 2nd free-free bending response at some test Mach numbers. As shown in the figures, at different Mach numbers, the dynamic bending responses were different. Fig 15 and 16 showed the plot of the peak values of the two modes' response power spectral density versus Mach numbers. It was shown that at different Mach numbers, the variation of the peak value of the free-free bending response power spectral density can be up to 14.4 times. Although the second-order aerodynamic damping was zero, it had a limited effect on the second-order dynamic bending response amplitude in this test condition.

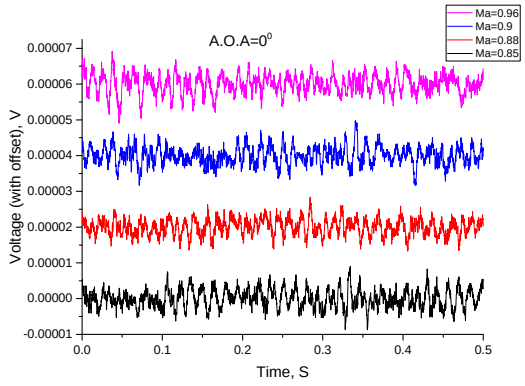


**Fig 9.** Dynamic response of bending at AoA=0°

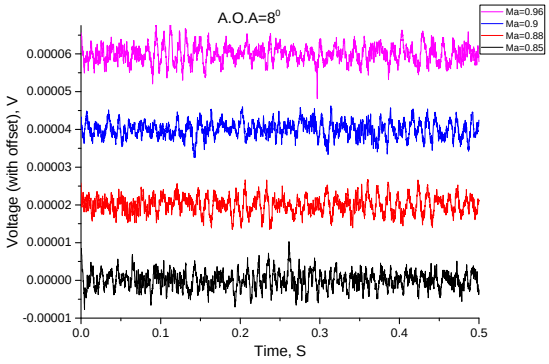


**Fig 10.** Dynamic response of bending at AOA=8°

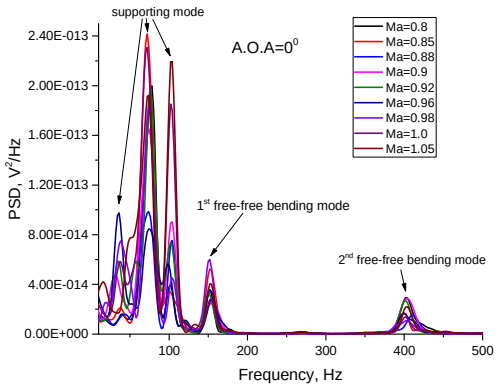


**Fig 11.** Power spectral density of the dynamic response, AoA=0°

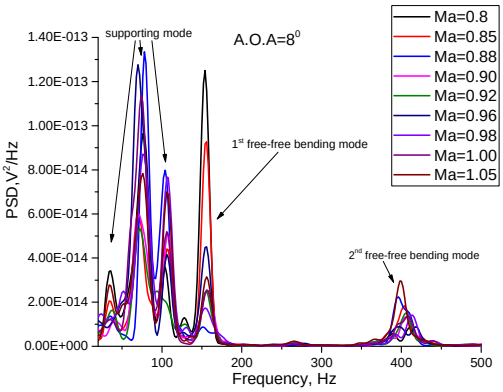


**Fig 12.** Power spectral density of the dynamic response, AOA=8°

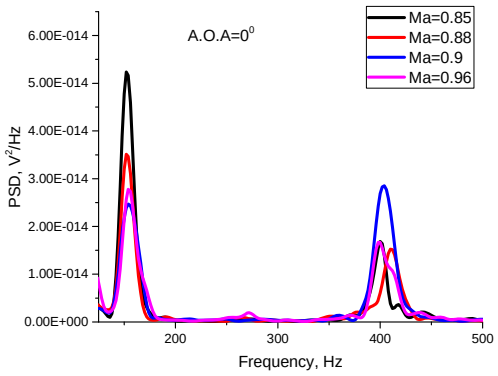


**Fig 13.** Power spectral density of the free-free bending response, AoA=0°

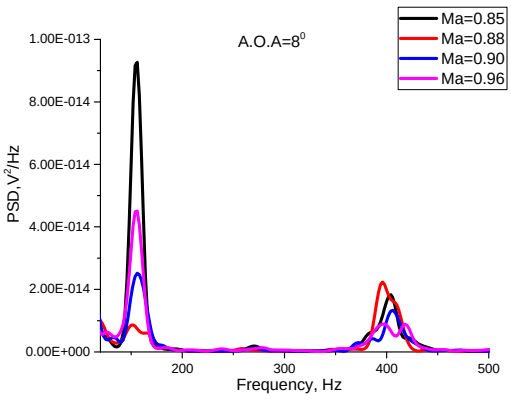


**Fig 14.** Power spectral density of the free-free bending response, AoA=8°

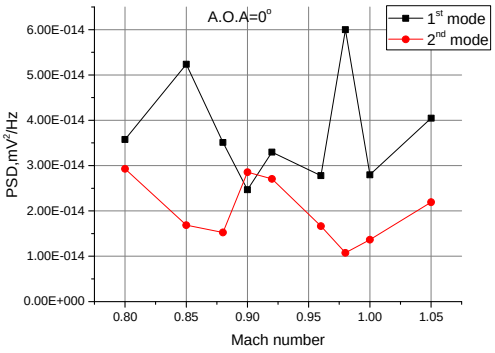


**Fig 15.** Peak value of the bending response PSD, AoA=0°

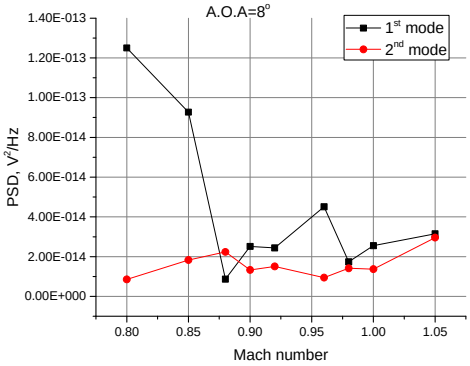


**Fig 16.** Peak value of the bending response PSD, AoA=8°

## 6. Conclusion

The aerodynamic damping and buffet response of a hammerhead launch vehicle were tested at the angles of attack of 0° and 8° and Mach numbers of 0.8 to 1.2 using an aeroelastic scaled model. The aeroelastic scaled model simulates the mass, stiffness and aerodynamic characteristics of the full-scale vehicle.

The aerodynamic damping of the model vibrating in the 1st and 2nd free-free bending mode were measured respectively by exciting the model at the corresponding modal frequency with an electromagnetic shaker. The aerodynamic damping dip can be found in both the 1st and 2nd free-free bending mode at the two tested angles of attack. The dip was at the Mach number of 0.88 for the 1st mode, and at the Mach number of 0.9 for the 2nd mode. The aerodynamic undamping was found at the second free-free bending mode at Ma=0.9 and AOA=8°, and the value was zero.

The buffet response was also tested by measuring the dynamic bending response under the flow exciting. Three supporting modes and two free-free bending modes were excited by the flow. At different Mach numbers, the variation of the peak value of the free-free bending response power spectral density can be up to 14.4 times. Although the second-order aerodynamic damping was zero at Ma=0.9 and AOA=8°, it had a limited effect on the second-order dynamic bending response amplitude in this test condition.

## References

1. Hanson, Perry W.; and Doggett, Robert V., Jr.(1962). ”Wind-Tunnel Measurements of Aerodynamic Damping Derivatives of a Launch Vehicle Vibrating in Free-Free Bending Modes at Mach Numbers From 0.70 to 2.87 and Comparisons With Theory”. NASA TN D-1391.
2. Hanson, Perry W.; and Doggett, Robert V., Jr.(1963). “Aerodynamic Damping of a 0.02-Scale Saturn SA-1 Model Vibrating in the First Free-Free Bending Mode”. NASA TN D-1956.
3. FENG Mingxi, LIU Yumin, JIA Quyao, FU Guangmin(1990). “Experiments on Aerodynamic Damping Using Elastic Models for Rockets Buffeting”. Beijing Institute of Aerodynamics, BG6-765, 1990.4
4. BAI Kui, FENG Mingxi(1990). “Aeroelastic Model and Buffet Experimental Technique”, Experiments and Measurements in Fluid Mechanics. Vol. 13, No.1, Mar, 1999
5. LIU Ziqiang, BAI Kui, MAO Guoliang, CUI Erjie(2002). “The Determination of Aerodynamic Damping on Hammerhead Launch Vehicles at Transonic Speeds”. Journal of Astronautics. Vol. 23, No. 6, Nov. 2002

6. LIU Ziqiang, CUI Erjie, BAI Kui, MAO Guoliang(2003). “Aerodynamic Undamping Phenomena of Structure Oscillating in Inviscid Flow”. ACTA MECHANIC SINICA. Vol. 35, No. 1, Jan. 2003
7. Chen JI, Feng LI, Ziqiang LIU, etc. The aerodynamic damping test of elastic launch vehicle model in transonic flow. In: Proceedings of the 64th International Astronautical Congress, IAC-13-D2.6.10; 2013.
8. Bisplinghoff, R. L.; Ashley, H.; and Halfman, R. L. (1955). Aeroelasticity. Addison-Wesley Pub. Co., Inc. (Cambridge, Mass.)